

# Simulation of carbon nanotube field effect transistors using NEGF

S Aravind<sup>1</sup>, S Shravan<sup>1</sup>, S Shrijan<sup>1</sup>, R Venkat Sanjeev<sup>1</sup>, B Bala Tripura Sundari<sup>2,3</sup>

<sup>1</sup> Department of Electronics and Communication Engineering, Amrita School of Engineering, Coimbatore, Amrita Vishwa Vidhyapeetham, Amrita University, India

<sup>2</sup> Associate Professor, Department of Electronics and Communication Engineering, Amrita School of Engineering, Coimbatore, Amrita Vishwa Vidhyapeetham, Amrita University, India

<sup>3</sup> b\_bala@cb.amrita.edu

**Abstract.** A nearest neighbour tight binding approximation for analysing the  $I$ - $V$  characteristics of ballistic CNTFETs is developed making use of the non-equilibrium green's function (NEGF) formalism. NEGF provides a matrix based computational since device description at the atomic level can be employed and multiple quantum phenomenon that are visible in real time can be effectively modelled. The proposed model involves zig-zag CNTs as the channel material with a 25nm channel length that uses a basis transformation to decouple the channel Hamiltonian. Temperature dependence on the output characteristics of CNTFETs with varying chirality is also studied. All simulations are carried out on MATLAB.

## 1. Introduction

Silicon has served the electronics industry since its introduction in 1947[1]. Thereon, in accordance with Moore's law, there has been a constant miniaturization in the device size while deriving increased performance. This has been possible due to scaling down of transistors. Recent research has shown that detriment of scaling has been evident. 1) Inability in proportionally scaling down the threshold voltage with channel length. 2) Need for scaling down the gate oxide thickness along with channel length without causing higher leakage currents. 3) Unfavourable scaling of parasitic resistances and capacitances due to scaling of channel length leading to higher interconnect delays. 4) Short channel effects observed significantly weighs against the brighter side of scaling [2]. Investments in finding a suitable alternative for Si were futile until carbon nanotubes, one of the eight allotropes of carbon was invented in 1991[3]. With this invention, scientists have actively participated in theoretically analysing carbon based transistors and the results have been promising [4]. In this paper the surface potential values are obtained from an online simulator that self-consistently evaluates Poisson's equation with NEGF for a CNT FET for a channel length of 25nm [6]. The final current equation is derived using the tight binding model which takes into account the effect due to nearest neighbouring atoms alone to develop the Hamiltonian for the CNT channel. This approach is simple yet as effective as approximations considering effects due to atoms farther apart which are difficult to model [8]. Decoupling the Hamiltonian is carried out using a basis transformation [9].



## 2. Carbon Nanotubes

### 2.1. Physical Structures

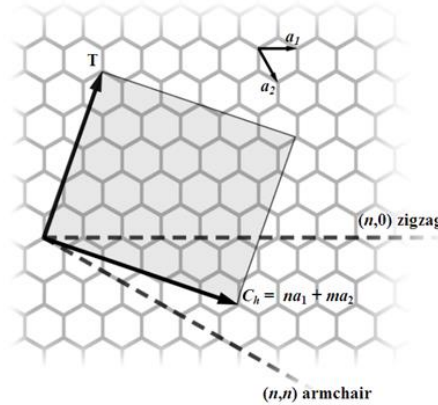


**Figure 1.** Chirality of a CNT

A carbon nanotube is visualized as a rolled up graphene sheet. The chiral vector provides information about the direction of the roll-up and for a chiral nanotube, this vector is defined as

$$\vec{C} = n\hat{a}_1 + m\hat{a}_2 \equiv (n, m) \quad (1)$$

with  $\hat{a}_1, \hat{a}_2$  being the basis vectors used to represent the graphene sheet as depicted in figure (1)

From the nearest neighbour tight-binding model using one  $2p_z$  orbital, the dispersion relation for graphene is as in equation (2)

$$E(\vec{k}) = \pm t \left( 1 + 4 \cos\left(k_x \frac{3a_{C-C}}{2}\right) \cos\left(k_y \frac{\sqrt{3}a_{C-C}}{2}\right) \cos^2\left(k_y \frac{\sqrt{3}a_{C-C}}{2}\right) \right)^{1/2} \quad (2)$$

From the specification of the chiral vector, the diameter can be computed as in equation (3)

$$d = \frac{\sqrt{3}a_{C-C}}{\pi} (n^2 + m^2 + nm)^{1/2} \quad (3)$$

The translation vector specifying the axis of the nanotube is given by

$$\vec{T} = \left(\frac{2m+n}{d}\right)\hat{a}_1 - \left(\frac{2n+m}{d}\right)\hat{a}_2 \quad (4)$$

Interesting feature of CNTs is that the threshold voltage is flexible with diameter of the nanotube.

$$v_{th} = \frac{0.43}{d} \quad (5)$$

Apart from the chiral nanotube described, there exist two different physical structures-zig-zag nanotubes represented by  $(n,0)$  and armchair nanotubes represented by  $(n,n)$ .

## 2.2 Model Structure

In this paper, coaxially gated zig-zag nanotubes are analysed for  $I$ - $V$  characteristics. Coaxial gating ensures that the channel surface potential and charge density along the circumferential path can be safely assumed to be same. The model structure employed is depicted in figure (2).

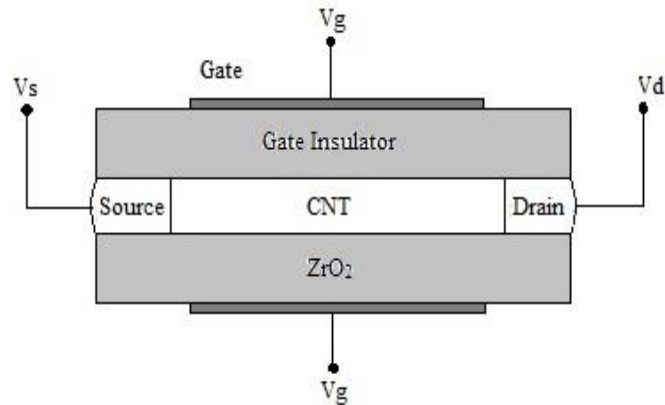


**Figure 2.** Modelled Structure of CNTFET

A 25nm zig-zag CNT with 1nm diameter acts as the channel material while a 20nm gate material is wrapped around the CNT. The gate insulator is  $ZrO_2$  with 1nm thickness and 25 as its dielectric constant. Inside the channel, the permittivity is assumed to be that of air ( $\epsilon_0$ ) and the source (S) and drain (D) contacts are 10nm in length with  $10^8$  /m as the n-doping concentration [5]. Since contacts are assumed to be semi-infinite metallic in nature the S/D regions are an extension of the nanotube.

## 3. NEGF Methodology

The NEGF methodology involves solving the retarded green's equation followed by the electron correlation green's equation.

$$G^R(E) = [EI - H - \Sigma_S(E) - \Sigma_D(E)]^{-1} \quad (6)$$

$$G^n(E) = G^R(E) \Sigma^{in} G^A(E) \quad (7)$$

The Hamiltonian matrix  $H$  in equation (6) is formulated using nearest neighbourhood tight binding approach as given in [5]. The channel surface potential forms the diagonal elements of the Hamiltonian and the self-consistent potential is obtained from [6]. Invariant potential along the circumference in coaxial gating allows decoupling of CNT lattices into a few single dimensional modes that contribute to transport is determined by performing suitable basis transformation to channel Hamiltonian. This transformation reduces the size of the channel Hamiltonian and so offers reduction in computational time [9].

$G^A(E)$  is the advanced green's function which is conjugate transpose of  $G^R(E)$ .  $\Sigma_{S,D}(E)$  are the contact self-energies of S/D respectively. Equation (7) gives the number of electrons in the device.

$$\Sigma^{in} = \Gamma_S f_S + \Gamma_D f_D \quad (8)$$

Equation (8) gives details about the strength of the contacts in providing electrons, while the factor  $\Gamma$  stands for the broadening function representing the strength of the coupling between the contacts and the device.

$$\Gamma_{S,D}(E) = i[\Sigma_{S,D} - \Sigma_{S,D}^+] \quad (9)$$

where  $\Sigma^+$  stands for conjugate transpose of  $\Sigma$ .

Using equation (6-9), the drain current can be computed as

$$I_d = \frac{4q}{h} \int_{-\infty}^{\infty} T(E) [f(E - \varepsilon_S) - f(E - \varepsilon_D)] dE \quad (10)$$

with the transmission probability function defined as

$$T(E) = trace[\Gamma_S G^R \Gamma_D G^A] \quad (11)$$

The factor of 4 appearing in equation (10) accounts for both the spin of electrons and the valley degeneracy.  $\varepsilon_S, \varepsilon_D$  are the fermi levels of S/D contacts [7].

#### 4. Simulation results and discussion

Following the approach discussed in section 3 the  $I$ - $V$  characteristics of the SW-CNTFET has been obtained for four different temperatures (273K, 300K, 323K, 373K) and two different chirality ((13,0), (17,0)). The characteristics are obtained for four different gate voltages starting from 0.2V with a scale of 0.2 till 0.8V. For the chosen physical configuration of the CNT the threshold voltage was fixed at 0.4V for chirality 13 and 0.34 for chirality 17 in accordance with equation (3, 5). The  $I$ - $V$  characteristics of a SW-CNTFET are very similar to that of a Si MOSFET in terms of the initial linear rise and further saturation but the current produced for a certain gate and drain voltage is considerably higher in a CNTFET. However temperature seems to have a very marginal effect over the current produced. For a 100K rise in temperature the drain current increases by 10 $\mu$ A.

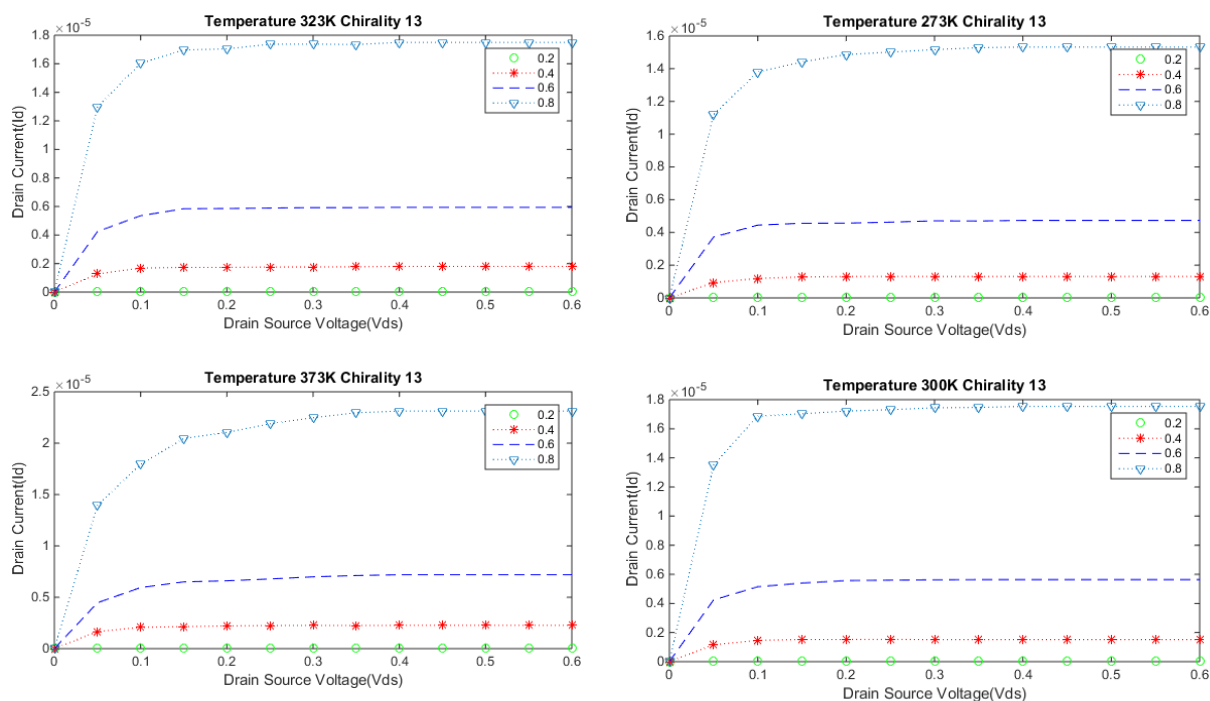


**Figure 3.** I-V Characteristics of a (13, 0) CNTFET  $V_g = 0.2, 0.4, 0.6$  and  $0.8$  at 273K, 300K, 323K and 373K.

From figure (4), at 300K for a CNTFET of chirality 13 the drain current for a gate voltage of 0.6V is  $5.66\mu\text{A}$  whereas a CNTFET of chirality 17 at the same electrical conditions produces a current of  $7.096\mu\text{A}$ . There is a rise in current by about  $1.436\mu\text{A}$  for a rise of  $0.32\text{nm}$  in diameter of the channel CNT.

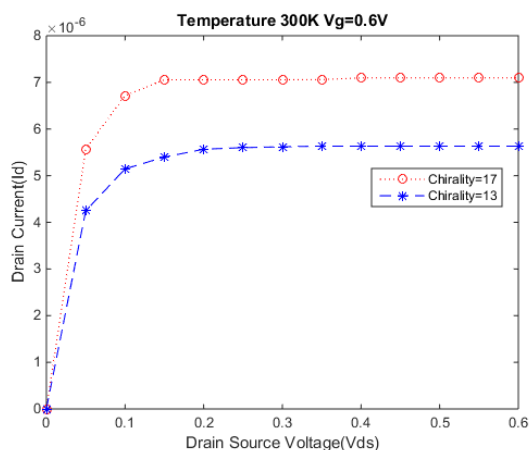


**Figure 4.** I-V Characteristics of a chirality 17 and chirality 13 CNTFET at 300K and  $V_g=0.6\text{V}$

**Table 1** Drain current for various chirality and temperatures

| <b>Chirality 13</b>        |                            |                            |                            |                            |
|----------------------------|----------------------------|----------------------------|----------------------------|----------------------------|
| <i>Temp/ V<sub>g</sub></i> | <i>V<sub>g</sub> = 0.2</i> | <i>V<sub>g</sub> = 0.4</i> | <i>V<sub>g</sub> = 0.6</i> | <i>V<sub>g</sub> = 0.8</i> |
| 273K                       | 0.18nA                     | 1.3μA                      | 4.73μA                     | 15.733μA                   |
| 300K                       | 6.51nA                     | 1.512μA                    | 5.633μA                    | 16.53μA                    |
| 323K                       | 9.65nA                     | 1.801μA                    | 5.94μA                     | 17.58μA                    |
| 373K                       | 16.64nA                    | 2.263μA                    | 7.19μA                     | 23.13μA                    |
| <b>Chirality 17</b>        |                            |                            |                            |                            |
| <i>Temp/ V<sub>g</sub></i> | <i>V<sub>g</sub> = 0.2</i> | <i>V<sub>g</sub> = 0.4</i> | <i>V<sub>g</sub> = 0.6</i> | <i>V<sub>g</sub> = 0.8</i> |
| 273K                       | 1.56nA                     | 1.5μA                      | 7.5μA                      | 17.46μA                    |
| 300K                       | 6.86nA                     | 1.602μA                    | 6.47μA                     | 17.858uA                   |
| 323K                       | 9.89μA                     | 2.9μA                      | 6.96μA                     | 18.246μA                   |
| 373K                       | 16.99nA                    | 3.442μA                    | 7.68μA                     | 24.654μA                   |

Fixing the chirality directly fixes the diameter of the CNT. Changing the chirality from 13 to 17 increases the diameter from 1.01nm to 1.33nm. Further the diameter decides the amount of electrons flowing through the tube. Table 1 presents the current  $I_d$  for varying temperatures and chirality of (13,0) and (17,0) and it is indisputable that the drain current by the CNTFET relies in the chirality of the CNT. Current obtained for (13, 0) CNTFET operating at  $V_g=0.8V$  and 300K is 16.53μA and current reported using numerical methods is 15μA [12].

## 5. Conclusion

Nearest neighbour tight binding modelling technique proves to be an effective way to yield a platform to analyse the  $I$ - $V$  characteristics of zig-zag CNTFET. A CNTFET was modelled with a channel approximation- nearest neighbour tight binding and with semi-infinite metal contacts using NEGF approach. Performing the basis transformation to decouple the CNTFET reduces the size of the Hamiltonian and the computational time in MATLAB. The mathematical models obtained in the process can be translated into HSPICE libraries to implement circuit level models and analyse the real time circuit performance of the transistor. HSPICE models can be optimized to suite a particular circuit or to perform optimally for any requirement.

## References

- [1] M. Riordan, L. Hoddeson and C. Herring, "The invention of transistor," *Rev. of Modern Phys.*, The American Physics Society, Vol. 71, No.2, 1999.
- [2] Chopra, Shivani, and Subha Subramaniam. "A review on challenges for MOSFET scaling," *Int. J. Innovative Science, Engineering and technology*, Vol.2, Issue 4, April, 2015.
- [3] S. Iijima and T. Ichihashi, "Single-shell carbon nanotubes of 1-nm diameter," *Nature*, 363, pp. 605- 7, 1993.
- [4] L. Rispal and U. Schwa Ike, "Carbon: the future of nanoelectronics," *Int. Conf. on Signal, Circuits and Systems*, 2009.
- [5] M. Shin, "Non-equilibrium green's function approach to three-dimensional carbon nanotube field effect transistor," *J. Korean Phys. Soc.*, Vol. 52, No.4, April 2008, pp. 1287-91.
- [6] Neophytos Neophytou, Shaikh S. Ahmed, POLIZZI ERIC, Gerhard Klimeck and Mark Lundstrom (2016), "CNTFET Lab," <https://nanohub.org/resources/cntfet>. (DOI: 10.4231/D3M90243W).
- [7] J. Guo and M.S. Lundstrom, "*Nanoscale transistors device physics, modeling and simulation*," Springer International Edition, 2008.
- [8] S. Datta, "*Quantum transport: atom to transistor*," Cambridge University Press, Cambridge, UK,

2005.

- [9] J.Guo, "Carbon nanotube electronics: modeling, physics and application," Ph.D Thesis, Purdue University, 2004.
- [10] S. Datta, "*Electronic transport in mesoscopic systems*," Cambridge: Cambridge University Press, UK, 1995.
- [11] R. Sreenath and B. Bala Tripura Sundari, "Modelling and performance comparison of graphene and carbon nanotube based fets," *ARPJ. Engg. and Appl. Sciences*, Vol.10, No.9, 2015.
- [12] Fedawy, Mostafa et al. "I-V Characteristics Model For Ballistic Single Wall Carbon Nanotube Field Effect Transistors (SW-CNTFET)", *IEEE Int. Conf. on Electronics Design, Systems and Applications*, 2012.